TISSUE ENGINEERING: Part A
Volume 19, Numbers 1 and 2, 2013

DOI: 10.1089/ten.tea.2011.0408

Dissecting the Role of Human Embryonic Stem Cell–Derived Mesenchymal Cells in Human Umbilical Vein Endothelial Cell Network Stabilization in Three-Dimensional Environments

Nolan L. Boyd, Ph.D.,[1] Sara S. Nunes, Ph.D.,[2] Laxminarayanan Krishnan, Ph.D.,[1,*] Jenny D. Jokinen, M.S.,[1] Venkat M. Ramakrishnan, B.S.,[1] Amy R. Bugg, B.S.,[1,3] and James B. Hoying, Ph.D.[1]

The microvasculature is principally composed of two cell types: endothelium and mural support cells. Multiple sources are available for human endothelial cells (ECs) but sources for human microvascular mural cells (MCs) are limited. We derived multipotent mesenchymal progenitor cells from human embryonic stem cells (hES-MC) that can function as an MC and stabilize human EC networks in three-dimensional (3D) collagen-fibronectin culture by paracrine mechanisms. Here, we have investigated the basis for hES-MC-mediated stabilization and identified the pleiotropic growth factor hepatocyte growth factor/scatter factor (HGF/SF) as a putative hES-MC-derived regulator of EC network stabilization in 3D *in vitro* culture. Pharmacological inhibition of the HGF receptor (Met) (1 μm SU11274) inhibits EC network formation in the presence of hES-MC. hES-MC produce and release HGF while human umbilical vein endothelial cells (HUVEC) do not. When HUVEC are cultured alone the networks collapse, but in the presence of recombinant human HGF or conditioned media from human HGF-transduced cells significantly more networks persist. In addition, HUVEC transduced to constitutively express human HGF also form stable networks by autocrine mechanisms. By enzyme-linked immunosorbent assay, the coculture media were enriched in both angiopoietin-1 (Ang1) and angiopoietin-2 (Ang2), but at significantly different levels (Ang1 = 159 ± 15 pg/mL vs. Ang2 = 30,867 ± 2685 pg/mL) contributed by hES-MC and HUVEC, respectively. Although the coculture cells formed stabile network architectures, their morphology suggests the assembly of an immature plexus. When HUVEC and hES-MC were implanted subcutaneously in immune compromised Rag1 mice, hES-MC increased their contact with HUVEC along the axis of the vessel. This data suggests that HUVEC and hES-MC form an immature plexus mediated in part by HGF and angiopoietins that is capable of maturation under the correct environmental conditions (e.g., *in vivo*). Therefore, hES-MC can function as microvascular MCs and may be a useful cell source for testing EC–MC interactions.

Introduction

The microvasculature is principally composed of two cells: the endothelium (endothelial cell [EC]) that provides the perfusion conduit and mural cells (MCs) (i.e., pericytes) that provide the structural support.[1] A large body of work has examined the formation of the vasculature from early developmental sources (for reviews see [2,3]) and shown that the endothelium originates from the mesodermal germ layer.[4–6] However, vascular MCs (i.e., smooth muscle and pericytes) have multiple developmental origins (for reviews see[7,8]). MCs of the cranial vasculature and cardiac outlet tract originate from neural crest[9,10] and coronary MCs derive from proepicardium[11,12] while most other MCs are of mesoderm origin.[13,14] Smooth muscle cells are easily identifiable as they form concentric layers surrounding arteries and veins[15] while expressing multiple contractile proteins, such as α-smooth muscle actin, smooth muscle-myosin heavy chain, smooth muscle-22α, and calponin.[13,16,17] In contrast, pericytes of the microvasculature have historically been identified by position on the vessel[18,19] as protein marker expression is species, developmental stage, and vascular bed dependent.[20] *In vitro*, cells commonly used to model pericytes are transformed mouse embryonic mesenchymal cells (10T1/2)[21] and perivascular cells isolated from the brain or retina.[22,23] Although perivascular cells have been derived from mouse and human embryonic stem cells, most vascular characterization has focused on functioning as smooth muscle (e.g., arterial)

[1]Cardiovascular Innovation Institute, University of Louisville, Louisville, Kentucky.
[2]Toronto General Research Institute, University Health Network, Toronto, Canada.
[3]Department of Bioengineering, University of Louisville, Louisville, Kentucky.
*Current affiliation: Georgia Institute of Technology, Parker H. Petit Institute for Bioengineering and Biosciences, Atlanta, Georgia.

rather than at the microvascular level.[24,25] An additional interesting characteristic of microvascular MCs described in the literature for over 40 years[26–30] is their phenotypic plasticity allowing them to differentiate along multiple lineages similar to adult mesenchymal stem cells (MSCs).[31,32] Recently, it was proposed that some portion of perivascular cells may be the source of MSCs.[33]

A stable microvasculature is required to maintain homeostasis in native tissue and is an essential technical hurdle for the engineering of clinically relevant-sized organ replacements.[34] Although immature vascular networks can form from EC alone, they tend to be leaky, unstable, and prone to regression.[35,36] Microvascular maturation requires the interaction between EC and MC for the assembling vasculature to progress to the mature state capable of providing for a tissue's metabolic needs.[37] Several mechanisms have been identified as mediating stages of microvascular assembly, such as platelet-derived growth factor (PDGF)-B,[37] transforming growth factor (TGF)β,[38,39] and angiopoietin-1/−2 (Ang1, Ang2),[40–42] yet it is unclear how EC and MC interact to form stable architectures. One of the difficulties of investigating EC–MC interactions is a lack of mural progenitor cells of human origin that can undergo the different stages of assembly from recruitment to mature integration.[35] We have used human embryonic stem cells (hESC) to derive multipotent mesenchymal cells (hES-MC) that we have shown are myogenic, osteogenic, and chondrogenic,[43] are responsive to PDGF-B and TGFβ1 signaling, and stabilize EC networks in three-dimensional (3D) collagen-fibronectin (Fn) gels by both paracrine and direct heterotypic contact.[44] Because these cells demonstrated multiple functional characteristics of microvascular MCs, we hypothesized that they may be MC precursors.

To test this hypothesis we further investigated the ability of hES-MC to interact with and stabilize EC networks. In this study we show that hES-MC and ECs form immature vascular plexus-like networks that (1) are stabilized by hepatocyte growth factor/scatter factor (HGF/SF), (2) differentially express Ang1 and Ang2, and (3) hES-MC integrate into EC networks *in vivo* similar to native MCs.

Materials and Methods

Reagents

Antibodies. Antibodies were purchased from the following sources: CD146 (550315; BD Biosciences), Cx43 (SAB4501174; Sigma), Tie2-Fc (313-TI) and IgG-Fc (110-HGm) from R&D Systems, NG2 (AB5320) and Met (05–1049) from Millipore, Akt (9272) and Phospho-Akt (4058) from Cell Signaling Technology, and EphrinB2 (SC-1010) and IgG_{2b} isotype control (SC-3879) from Santa Cruz Biotechnology. UEA1-Fluorescein (FL-1061) was purchased from Vector Laboratories. *Growth Factors:* hHGF (294-HG), mHGF (2207-HG), Ang1 (923-AN), VEGF (293-VE), and bFGF (233-FB) were purchased from R&D Systems. *Inhibitors:* Met inhibitor SU11274 (4101) was purchased from Tocris Bioscience. PI3K inhibitors Wortmannin (681675) and LY294002 (440202) were purchased from EMD Chemicals/Calbiochem. *ELISA:* HGF (DHG00), Ang1 (DANG10), and Ang2 (DANG20) ELISA Quantikine kits were purchased from R&D Systems. *Reagents:* All reagents were purchased from Sigma-Aldrich unless noted otherwise.

Cell culture

hES-MC were derived from H9 (WiCell) hESC and subsequently cultured in EGM2-MV (Lonza) as described previously.[43] Human umbilical vein endothelial cells (HUVEC) were purchased commercially and cultured in EGM2-MV (Lonza). HepG2 were a kind gift of Dr. Steven Stice of the Animal and Dairy Science Department at the University of Georgia. HepG2 were cultured in DMEM high glucose, 10% FBS (Hyclone-Thermo Fisher), 1×pen/strep, and 1×L-glutamine (Invitrogen). Cells were cultured at 37°C in 5% CO_2.

3D collagen-Fn constructs and experimental media

For all *in vitro* experiments, HUVEC alone or in coculture with hES-MC were cultured in experimental media (EM) consisting of DMEM/F12, 1×pen/strep, 1×L-glutamine (Invitrogen), 1 μM insulin, 5 μg/mL transferrin, 0.2 mM ascorbate (Sigma-Aldrich), 40 ng/mL VEGF, and 40 ng/mL bFGF.[44] For *in vitro* network formation assays, HUVEC alone or HUVEC with hES-MC were seeded into 1.5 mg/mL rat tail collagen I (BD Biosciences) with 90 μg/mL fibronectin (Sigma-Aldrich) at a concentration per mL of 10^6:0.2×10^6 (EC:hES-MC). Two hundred microliters of cell-gel solution was transferred per well of a 48-well plate (BD Falcon) and polymerized at 37°C for 30 min and then EM was added.

Viral vectors and transduction

For stable expression of GFP, hES-MC were transduced with pBMN-I-GFP retrovirus (Addgene plasmid 1736; Gary Nolan Lab) as described previously.[44] HUVEC were stably transduced with DsRed-Express pMXs retrovirus (Addgene plasmid 22724; Toshio Kitamura Lab)[45] as described previously.[44] HepG2 or HUVEC were stably transduced with pBABE-puro-Empty control (Addgene plasmid 1764; Weinberg Lab[46]) or pBABE-puro-HGF (Addgene plasmid 10901; Weinberg Lab[47]). Viral particles were generated using Phoenix ampho-packaging cells (Orbigen) as previously described.[44] The pBABE-puro vector backbone contains a puromycin antibiotic-resistant gene cassette allowing nontransduced cells to be killed off by the addition of puromycin to the culture. Because cell lines have different tolerances to puromycin, we determined the concentration to use for selection on HepG2 and HUVEC by performing a puromycin dose curve from 0 to 10 μg/mL on nontransduced cells. The lowest puromycin concentration that killed 100% of the nontransduced cells within 3 days was selected (10 μg/mL and 1 μg/mL of puromycin [Invitrogen] for HepG2 and HUVEC, respectively). All recombinant DNA work was approved by the University of Louisville Institutional Biosafety Committee.

Flow cytometry

HUVEC or hES-MC were incubated with Accutase (Innovative Cell Technologies), a nonenzymatic dissociation buffer, followed by three successive incubations on ice for 30 min each of 5% normal goat serum (Fisher Scientific), anti-Met or IgG_{2b} isotype control antibody, and goat anti-mouse PE or goat anti-rabbit PE secondary antibody. Cells were quantified on a BD FACScaliber with CellQuest Pro software (BD Biosciences).

Quantitative real-time polymerase chain reaction

Samples were processed for total RNA isolation using Qiagen Qiashredder and RNeasy kit according to the manufacturer's instructions (Qiagen). cDNA was generated using AfinityScript QPCR per the manufacturer's instructions (Agilent Technologies). Each sample was processed with and without reverse transcriptase (RT). Quantitative RT–polymerase chain reaction (PCR) was performed on each sample for expression of human *HGF* (forward: 5′-CAGCGTTGGG ATTCTCAGTAT-3′, reverse: 5′-CCTATGTTTGTTCGTGTT GGA-3′) and *ACT-β* loading control (forward: CTGTGGC ATCCACGAAACTA, reverse: AGTACTTGCGCTCAGGA GGA) using a Corbett Rotor Gene 6000. Samples were quantified by Comparative CT[48] and normalized to *HGF* transduced cells.

Fluorescence microscopy

For fluorescence microscopy, HUVEC were treated with UEA1-fluorescein (Vector Labs) or transduced with DsRed while hES-MC were stably transduced to express GFP as described earlier. The cells were fixed with 4% PFA (Electron Microscopy Sciences) for 10 min, they were washed with phosphate-buffered saline (PBS), and images were acquired on an Olympus IX71 inverted fluorescence microscope (Olympus). Confocal image stacks of construct implants were obtained using sequential channel acquisition for GFP and DsRed with 1 μm step size at 40× magnification using an Olympus BX61SWI laser scanning confocal microscope controlled by FluoView software (Olympus).

Trans-well migration assay

Trans-well inserts with 8-μm pore size (BD Biosciences) were coated with 50 μg/cm^2 of fibronectin (Sigma-Aldrich) and incubated for 2 h at 37°C and then coated with 0.1% gelatin (Sigma-Aldrich) for an additional 2 h at 37°C before plating HUVEC at 3.3×10^5/cm^2 in a base media of DMEM/F12 with 0.5% FBS (Invitrogen).[49] HUVEC were subjected to the following conditions for 12 h: negative control (base media only), base media with Ang1 (50 ng/mL), Ang1 with Tie2-Fc (20 μg/mL), or Ang1 with IgG-Fc (20 μg/mL). The transwell membrane was fixed in 4% PFA for 10 min; the inside of the well was swabbed with a Q-tip and rinsed twice with PBS and then incubated in 1 μg/mL DAPI (4′,6-diamidino-2′-phenylindole, dihydrochloride; Thermo-Scientific). The membrane was cut from the well and placed on a glass slide, treated with anti-fade mounting media Prolong Gold (Invitrogen), and covered with a glass slip. Ten random fields were taken from each condition; nuclei were counted and quantified.

Conditioned media experiments

For conditioned media experiments, hES-MC or transduced HepG2 (pBABE-puro-Empty or pBABE-puro-HGF; see "Viral vectors and transduction" section) were plated into 48-well tissue culture plates at 2×10^5/well for each day of the experiment (i.e., 5 wells/cell line for experiments lasting 5 days). Twenty-four hours after plating, a well was washed 2× with PBS and 200 μL of EM was added. Negative control wells did not contain cells but had an equivalent volume of EM added for the same time period. Fresh conditioned media or negative control was added to the HUVEC experimental wells daily. For Tie2 experiment, CM from one well of hES-MC was divided into half with one sample incubated with IgG-Fc and the other with Tie2-Fc at 20 μg/mL (R&D Systems). CM samples and non-CM negative control were incubated at 37°C for 30 min before adding to HUVEC. For HepG2 ± HGF CM, the experiment was performed as just described, but CM was generated from HepG2-Empty, HepG2-HGF, and non-CM (i.e., no cells but incubated in same tissue culture plate for 24 h). Fluorescence images of HUVEC-DsRed were acquired daily with quantification of networks performed on last day of experiment (i.e., day 7). Human HGF protein expression from hES-MC, and transduced HUVEC and HepG2 was performed using human HGF Quantikine Kit per the manufacturer's directions. Ang1 and Ang2 enzyme-linked immunosorbent assay (ELISA) was performed by collecting nonconditioned EM or EM conditioned from HUVEC/hES-MC coculture, HUVEC alone, or hES-MC alone in 3D collagen-Fn and assayed with the Quantikine kit per the manufacturer's instructions.

Inhibitor studies

Cytotoxicity (Cytotox-Fluor Assay; Promega), inhibitor dose, and equivalent maximum dimethyl sulfoxide (DMSO) volume controls were performed to determine the minimum inhibitor concentration to use. Cultures of HUVEC with hES-MC were treated with inhibitors at the noted concentration or an equivalent volume of DMSO at the beginning of the experiment (i.e., when media are added to the polymerized construct). Quantification of networks was performed as described in "Mono- and coculture network analysis" section. To test downstream Akt inhibition by Wortmannin and LY294002, HUVEC were serum starved for 4 h in DMEM/F12 with 0.5% FBS and then pretreated for 30 min with 10 μM Wortmannin, 50 μM LY294002, or DMSO negative control. Human HGF was added to the culture for 30 min and then samples were prepared for western blot for Phospho-Akt and Akt as described previously.[44]

HGF rescue of HUVEC networks

HUVEC alone were added to collagen-Fn gels and allowed to polymerize as described. EM was added without HGF (negative control) or with increasing doses of human or mouse HGF. Experiments lasted 7 days and networks were quantified as described in "Mono- and coculture network analysis" section.

HUVEC HGF autocrine regulation of network formation

HUVEC transduced and puromycin selected for expression of empty or HGF were placed into collagen-Fn gels as described and cultured for 7 days in EM. At the end of each experiment, networks were quantified as described in "Mono- and coculture network analysis" section.

In vivo *coculture implant*

HUVEC-DsRed and hES-MC-GFP were added to growth-factor-reduced Matrigel at a concentration of 2×10^6 and 0.4×10^6, respectively. Cell–Matrigel constructs were added to four-well Nunc IVF plates (Nunc) at 200 μL/well and polymerized for 30 min. EM was added and networks were allowed to form for 3 days. Constructs were then implanted

subcutaneously in the backs of Rag1 immune compromised mice (B6.129S7-*Rag1*^{tm1Mom}/J; Jackson Laboratories) for 1 week.[50] Animals were euthanized and constructs were harvested and fixed for 30 min in 4% PFA. Samples were washed with PBS and imaged by confocal microscopy as described. All animal studies were performed in accordance with the University of Louisville IACUC approval.

Mono- and coculture network analysis

For network analysis, constructs were imaged at 4× for two-dimensional (2D) fluorescence imaging and 20× and 40× for laser scanning confocal microscopy. For each 2D sample, 10 fields were acquired. For 3D confocal images, a minimum of five image stacks were acquired. Confocal image stacks were first imported into NIH ImageJ and converted to eight-bit grayscale; stack attributes were noted and saved for further processing in a commercial image processing software (Amira; Visage Imaging) as originally described by Krishnan *et al.*[51] Briefly, images were corrected for imaging depth, deconvolved, median filtered, and binarized (Supplementary Figs. S3 and S4; Supplementary Data are available online at www.liebertpub.com/tea). The connected components were evaluated in binarized images of both the HUVEC networks and the hES-MC. The locations of overlap between the two were then determined by calculating the volume common to both the images using a logical "and" function based on the description by Nunes *et al.*[52] The overlap volume represents the volume common to both the HUVEC networks and the hES-MC. This volume was then represented as a ratio of the total network volume and the total cell volume.

The 2D fluorescence images were first converted to grayscale, deconvolved, filtered, binarized, and size filtered in Matlab (MathWorks, Inc.). These binarized images were then imported into Amira to extract the medial skeleton of the networks. This skeletonized data were then parsed by a custom C++ program (WinFiber 3D; Musculoskeletal Research Labs, University of Utah, Salt Lake City, UT; http://mrl.sci.utah.edu/software/winfiber3d) as described earlier.[51,52] The coordinates from the skeletonized data were evaluated to obtain the total number of vessels, the number of branch points, the total number of end points, segment (section between two nodes: branch or end), and vessel lengths and diameters. The mean network (vessel) length, calculated from all images of the replicates of a treatment group, was used as the primary index of network stabilization and compared across groups for statistical significance.

Statistical analysis

Mean network lengths were compared between the various treatment groups using multiple one-way analysis of variance (ANOVA) or its nonparametric equivalent in SigmaStat (Systat) as appropriately indicated with each comparison (alpha = 0.05). The number of independent experiments is noted in the text as "$n = x$."

Results

Cell characterization

We have previously shown that hES-MC possess similar functionality to that of MSCs being osteogenic, chondrogenic, myogenic, and interact with EC.[43,44] The literature suggests that MSCs and perivascular cells may have a common lineage and are functionally interchangeable.[29,30] Therefore, we asked whether hES-MC express markers that can be associated with perivascular cells. In Figure 1A, hES-MC were found to be positive for CD146 (55%), NG2 (99%), EphB2 (90%), and Cx43 (91%). Because the pleiotropic molecule HGF is an angiogenic growth factor expressed by mesenchymal cells,[53] we then tested by ELISA whether hES-MC express HGF (Fig. 1B). When cultured in the defined EM as described in the "Materials and Methods" section, the hES-MC conditioned media were found to contain 5302 ± 1022 pg/mL (mean ± SE, $n = 3$) of HGF. We then tested whether HUVEC and hES-MC express the HGF receptor Met (Fig. 1C) and found that both cell types showed significant populations positive for Met (HUVEC = 56%; hES-MC = 75%). This data suggests that hES-MC posses multiple characteristics typically attributed to perivascular cells.

HGF/Met mediates EC network stability

From our previous work we have shown that hES-MC are capable of stabilizing HUVEC networks in 3D constructs *in vitro* by paracrine mechanisms.[44] However, it was unclear what mechanisms were responsible for these effects. Although VEGF and bFGF are potent angiogenic factors,[54] they are insufficient to induce human EC survival and network formation.[44,55] Therefore, other paracrine factors from hES-MC must be mediating the EC network stability. Because hES-MC express HGF, we tested what role it may contribute to the paracrine stabilization of EC (Fig. 2). HUVEC and hES-MC were combined in collagen-Fn gels and then exposed to the Met inhibitor SU11274[56,57] (1 μM) or an equivalent volume of DMSO at the initiation of coculture (Fig. 2A). At this dose, no cytotoxic effects were detected by Cytotox assay on either cell types (Supplementary Fig. S1). Addition of DMSO had no deleterious effect (*middle panel*) while blockade of Met by SU11274 resulted in disruption of network formation (*right panel*). One-way ANOVA indicated a significant effect on mean network length with SU11274 treatment compared with DMSO (Fig. 2B; $^*p = 0.001$, $n = 3$). If blockade of Met disrupted EC network formation, we reasoned that exogenous addition of HGF in the absence of hES-MC should rescue network formation (Fig. 3A). As expected, the negative control omitting HGF showed poor network formation (*first panel*), but the addition of 50 and 100 ng/mL of recombinant human HGF rescued network formation (*middle panels*). In agreement with what other labs have shown,[58] mouse recombinant HGF is not recognized by human Met resulting in networks paralleling the negative control (*last panel*). ANOVA analysis and pairwise comparison indicated that 50 and 100 ng/mL human HGF had a statistically significant effect on mean vessel length (MVL) compared with the negative control and mouse HGF ($^*p < 0.05$, $n = 3$) while no difference was detected between 50 and 100 ng/mL human HGF or the negative control and mouse HGF (Fig. 3B). Together these data suggest that HGF plays a significant role in the stability of EC networks mediated by hES-MC.

HGF paracrine and autocrine signaling stabilizes HUVEC networks

While blockade of Met and addition of exogenous recombinant HGF differentially mediated EC network

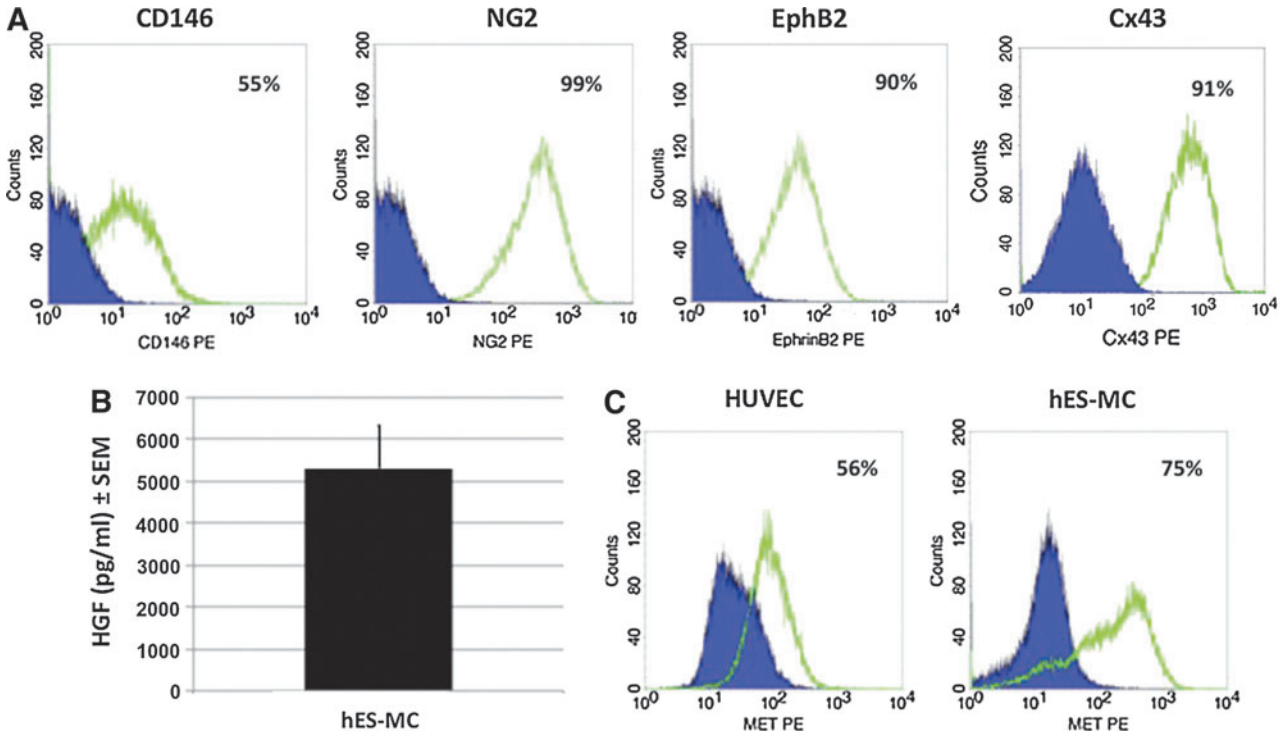

FIG. 1. Cell characterization. **(A)** Flow cytometry analysis of marker expression on human embryonic stem cells–mesenchymal cells (hES-MC). **(B)** hES-MC express HGF protein at a level of 5303 ± 1022 pg/mL as detected by ELISA. **(C)** Flow cytometry analysis of Met expression on human umbilical vein endothelial cells (HUVEC) and hES-MC. HGF, hepatocyte growth factor. Color images available online at www.liebertpub.com/tea

stability, it was unclear whether paracrine-mediated stability could be replicated by other cells. HepG2 are hepatocellular carcinoma epithelium that do not express HGF[59]; therefore, we stably transduced HepG2 with empty or human HGF retrovirus and selected for expression using 10 μg/mL puromycin. HGF gene transcription and protein expression were confirmed by PCR (Fig. 4A) and ELISA (>50,000 pg/mL), respectively (Fig. 4B). We then generated conditioned media from each cell or no conditioning negative control (Fig. 4C). Conditioned media from the empty transduced HepG2 showed more networks (*left panel*) than the non-CM negative control (*right panel*), but HUVEC exposed to HepG2 transduced to express HGF formed significantly more networks than the empty transduced cells (*middle panel*). Quantification of the formed networks showed a significant difference by one-way ANOVA in the networks formed by exposure to the paracrine release of HGF (Fig. 4D; $^*p < 0.001$, $n = 3$).

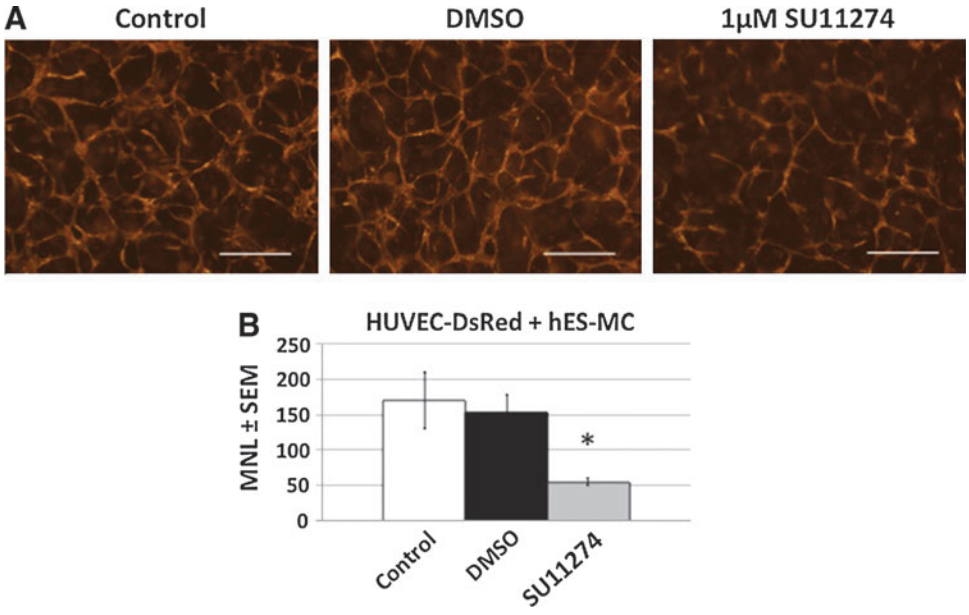

FIG. 2. Met blockade disrupts hES-MC-stabilized EC networks. **(A)** HUVEC and hES-MC coculture alone (*Control, left*) or treated with either dimethyl sulfoxide (DMSO) (*middle*) or Met inhibitor SU11274 at 1 μM (*right*). **(B)** Quantification of mean network length and one-way analysis of variance (ANOVA) indicated a significant effect of SU11274 (61 ± 2 μm) treatment compared with DMSO control (658 ± 200 μm) ($^*p = 0.001$, $n = 3$; 4×, scale bar = 250 μm). Color images available online at www.liebertpub.com/tea

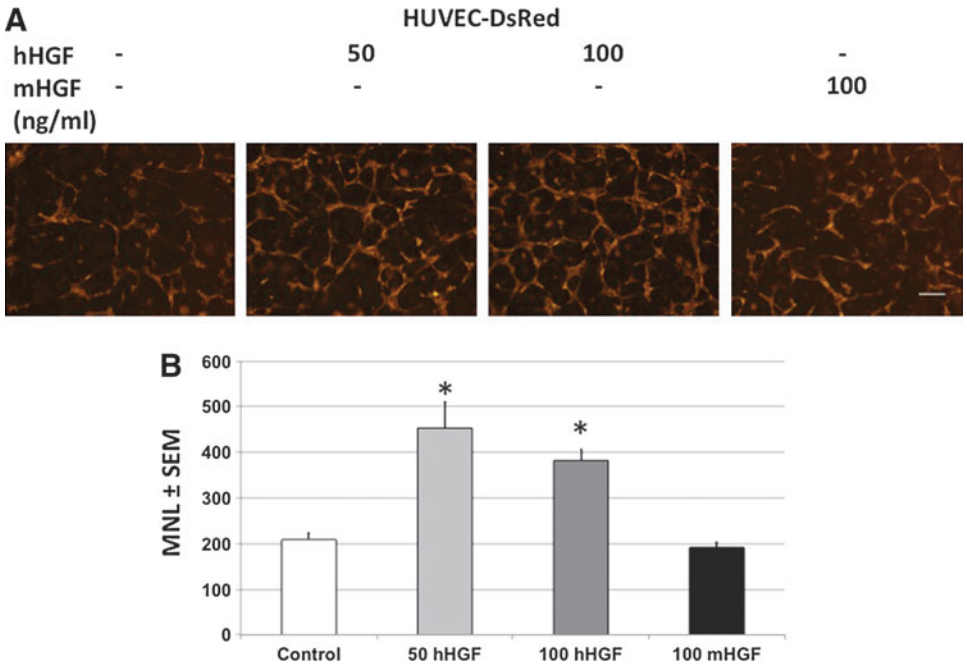

FIG. 3. Exogenous recombinant human HGF rescues EC networks. **(A)** HUVEC cultured in collagen-Fn gel were exposed to no treatment (*left*, 209 ± 16 μm), 50 or 100 ng/mL of human HGF (*middle*, 453 ± 56 μm and 382 ± 23 μm, respectively), or 100 ng/mL mouse HGF (*right*, 191 ± 12 μm). **(B)** Mean network length and one-way ANOVA indicate significant effect of treatment with human HGF on network formation (*$p < 0.05$, $n = 3$; 4×, scale bar = 250 μm). EC, endothelial cell. Color images available online at www.liebertpub.com/tea

HUVEC do not normally express HGF[60] (Fig. 5A); therefore, to test whether autocrine HGF expression by HUVEC could rescue network formation, we transduced HUVEC-DsRed with the same empty or HGF retroviral vectors used with the HepG2 and selected for expression with 1 μg/mL puromycin. ELISA-confirmed HGF protein expression was essentially absent in the empty transduced HUVEC but abundantly produced by the HUVEC transduced with the HGF vector (Fig. 5B; >80,000 pg/mL). HUVEC expressing the empty vector showed little network stability (Fig. 5A, *left panel*) while autocrine expressed HGF led to partial rescue of network formation and stability (*right panel*). Quantification of the formed networks showed a significant difference by one-way ANOVA in the networks formed by exposure to the autocrine release of HGF (Fig. 5C; *$p < 0.001$, $n = 3$). This data suggests that HGF can act as a significant paracrine/autocrine mediator of the stability of EC networks in 3D culture.

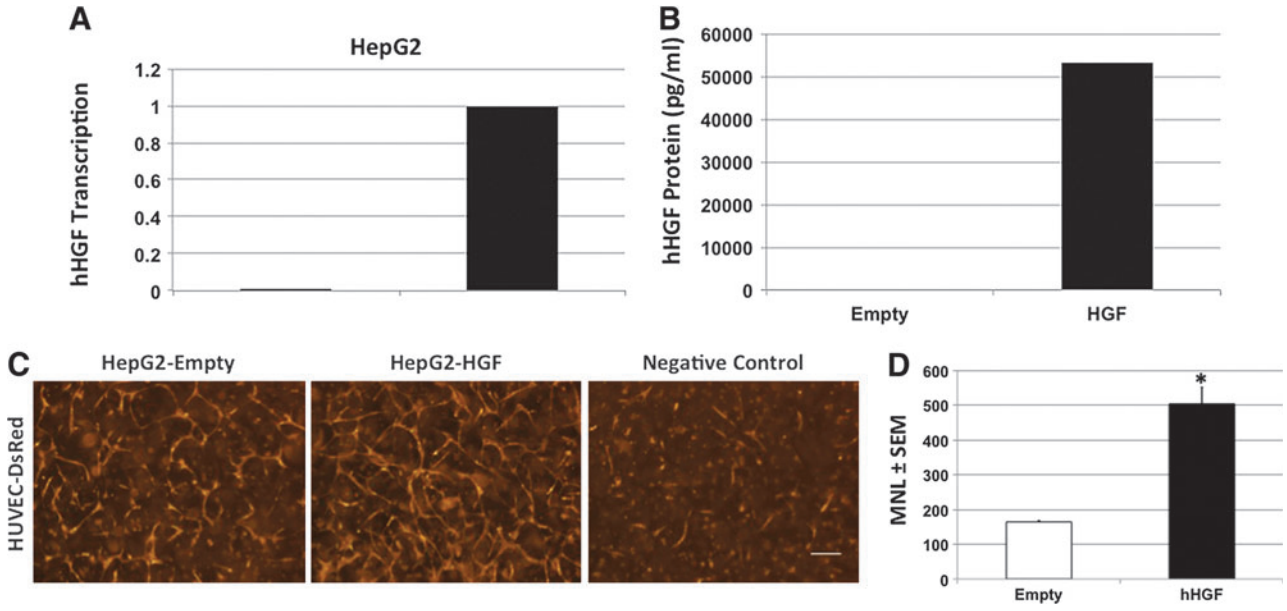

FIG. 4. HGF-conditioned media stabilize EC networks. **(A)** Non-HGF-expressing HepG2 were stably transduced with empty (*Empty*) or human HGF (*HGF*) retrovirus and transcription was confirmed by polymerase chain reaction. **(B)** HepG2 transduced to constitutively express HGF produced 53,072 pg/mL as detected by ELISA. **(C)** HUVEC cultured in collagen-Fn gel were cultured in HepG2-CM-expressing empty vector (*left*, 164 ± 4 μm), human HGF (*middle*, 503 ± 48 μm), or non-CM (*right*). **(D)** Mean network length and one-way ANOVA indicate significant effect of conditioning media with HepG2 expressing human HGF on network formation (*$p < 0.001$, $n = 3$; 4×, scale bar = 250 μm). Color images available online at www.liebertpub.com/tea

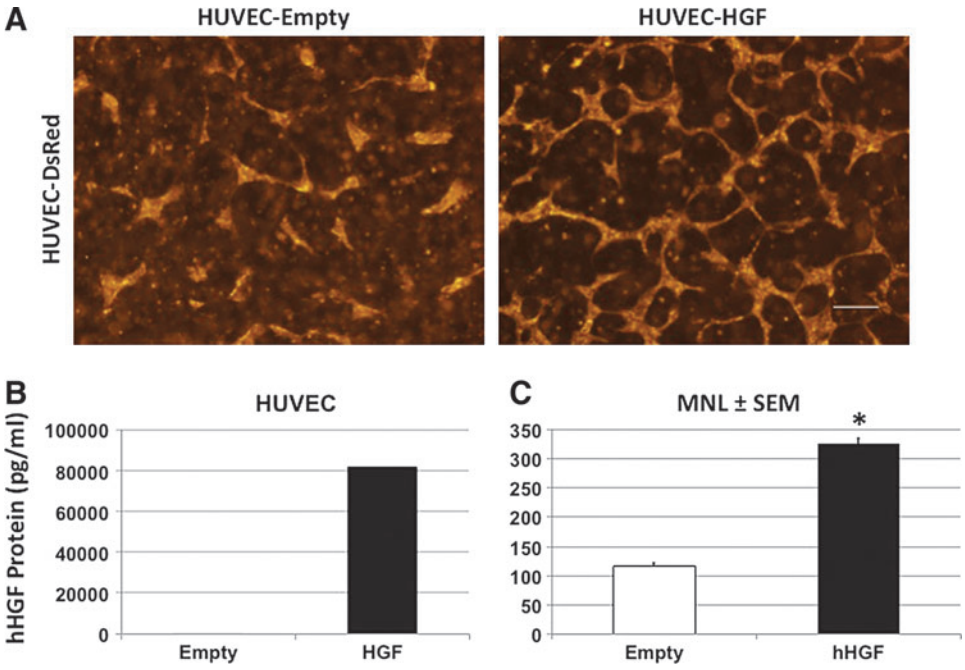

FIG. 5. HUVEC autocrine expression of HGF stabilizes networks. **(A)** HUVEC were stably transduced with empty (*left*, 116 ± 6 μm) or human HGF (*right*, 325 ± 10 μm) and cultured in collagen-Fn gel. **(B)** HUVEC transduced to constitutively express HGF produced 81,680 pg/mL HGF as detected by ELISA. **(C)** Mean network length and one-way ANOVA indicate significant effect of HUVEC autocrine expression of human HGF on network formation ($^{*}p < 0.001$, $n = 3$; 4×, scale bar = 250 μm). Color images available online at www.liebertpub.com/tea

PI3K/Akt mediates HUVEC network stability in 3D culture

Met is a tyrosine kinase receptor[61] and signals through the downstream PI3K/Akt, MAPK, and other pathways. Because of their roles in cell survival, angiogenesis, and tubulogenesis, we investigated whether PI3K/Akt and MAPK play roles in hES-MC-mediated EC network stability (Fig. 6A). While MAPK inhibitors PD98059 and U0126 had some effect on disrupting EC-hES-MC networks (data not shown), the PI3K/Akt inhibitors Wortmannin (10 μM, *top row*) and LY294002 (50 μM, *bottom row*) showed significant disruption of HUVEC networks compared with DMSO controls. Interestingly, the inhibitors primarily appeared to affect HUVEC survival (*first and third columns*) while showing modest effect on hES-MC survival (*second and fourth columns*). Treatment of HUVEC with either LY294002 (50 μM) or Wortmannin (10 μM) blocks phosphorylation of Akt induced by HGF (50 ng/mL) (Fig. 6B). This data suggests that the EC stabilizing effect of hES-MC paracrine signaling is at least partially mediated through the PI3K/Akt signaling pathway.

Ang1 and Ang2 expression in HUVEC-hES-MC coculture

Because angiopoietins play a role in vascular assembly,[62,63] we tested whether Ang1 and Ang2 were being expressed in the 3D environment of HUVEC/hES-MC coculture versus HUVEC alone versus hES-MC alone (Fig. 7). Fresh EM was added to each culture on day 2 and collected for ELISA analysis on day 4. EM is a defined media without the supplementation of Ang1 (Fig. 7A) or Ang2 (Fig. 7B) and the ELISA-indicated levels of 26 ± 5 pg/mL and 622 ± 101 pg/mL, respectively, was within the range of background for the assay. The coculture conditioned media (Co) contained levels of Ang1 and Ang2 at 159 ± 15 pg/mL and 30,867 ± 2685 pg/mL, respectively, that were statistically significantly greater than EM control ($^{*}p = 0.004$ and 0.01, respectively, $n = 3$). When cells were analyzed individually, HUVEC Ang1 expression was not different from the EM control (25 ± 4 pg/mL, *NS*) while hES-MC alone produced 100 ± 18 pg/mL, which was significantly greater than EM control ($^{\#}p = 0.02$) but significantly less than the coculture ($p = 0.004$). ELISA analysis of the same media samples for Ang2 indicated robust expression in the coculture media that was significantly greater than EM control (30,867 ± 2685 pg/mL, $^{\#}p = 0.01$). However, opposite to Ang1, HUVEC expressed a significantly greater amount compared with EM control (14,289 ± 1318 pg/mL, $^{*}p = 0.007$) but less than coculture ($p = 0.009$). For Ang2, hES-MC expression was not different from EM control (600 ± 144 pg/mL, *NS*). We then tested whether Ang1 and Ang2 mediate HUVEC network formation by exposing hES-MC conditioned media to the blocking antibody Tie2-Fc (20 μg/mL)[64,65] shown to inhibit angiopoietin activity[66] or IgG-Fc (20 μg/mL) control before adding it to HUVEC seeded in collagen-Fn gels. This concentration of Tie2-Fc inhibits HUVEC migration in a transwell assay when exposed to 50 ng/mL HGF while no effect on HUVEC migration is seen when exposed to an equivalent dose of IgG-Fc (Supplementary Fig. S2). As can be seen in Figure 7C (*left panel*), HUVEC exposed to control EM formed few networks while hES-MC CM containing IgG-Fc control generated networks similar to what we have previously reported[44] (*middle panel*). However, when Tie2-Fc was added to the CM (*right panel*) there was no difference in the capacity for HUVEC to form networks compared with IgG-Fc treatment. One-way ANOVA comparing the MVL of control to IgG-Fc- and Tie2-Fc-treated CM indicated a significant increase in network formation in the treated cultures (Fig. 7D; $^{*}p > 0.05$, $n = 3$) while network length from hES-MC CM treated with IgG-Fc or Tie2-Fc showed no significant difference (Fig. 7D; $p = 0.74$, $n = 3$). Although the Tie2-Fc antibody was able to block recombinant-HGF-mediated migration of HUVEC, it was unclear whether the lack of network disruption was due to the elevated levels of

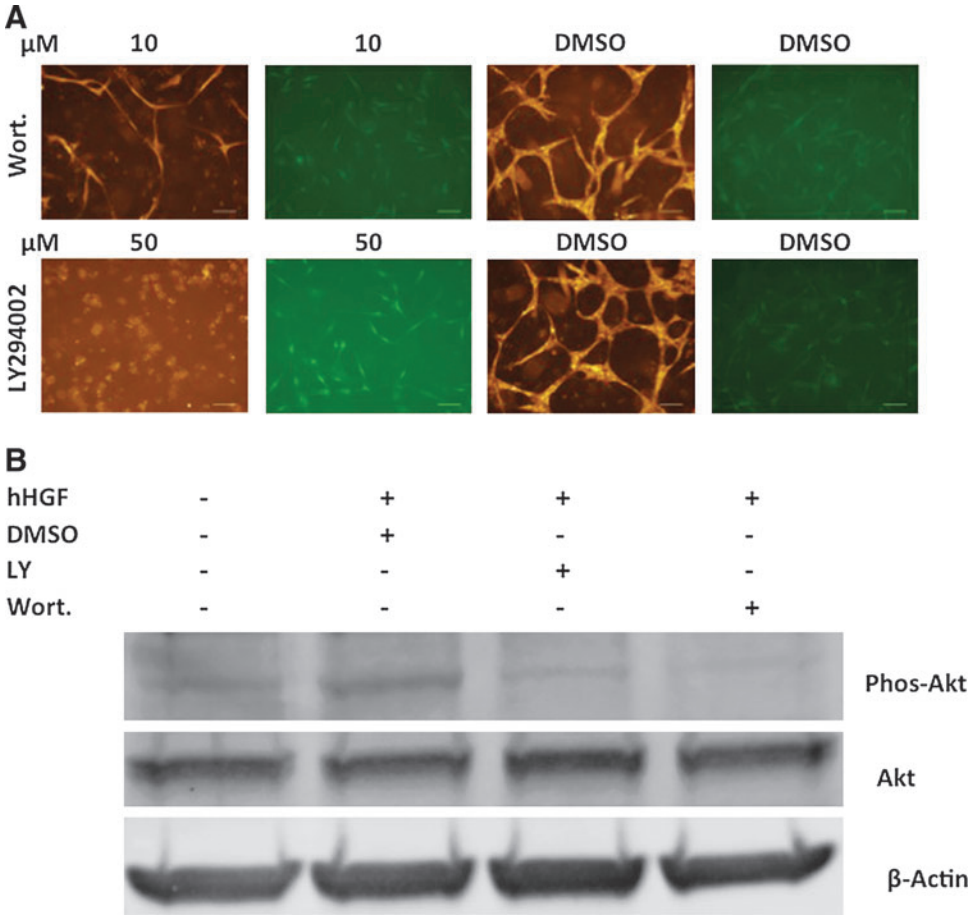

FIG. 6. PI3K/Akt inhibitors disrupt hES-MC-stabilized EC networks. **(A)** HUVEC and hES-MC were cocultured in collagen-Fn gels and treated with the PI3K/Akt inhibitors Wortmannin (10 μM, *top*), LY294002 (50 μM, *bottom*), or equivalent volumes of DMSO ($n = 3$; 4×, scale bar = 250 μm). **(B)** HUVEC exposed to HGF showed phosphorylation of Akt that was blocked by addition of Wortmannin (10 μM) or LY294002 (50 μM). Total Akt and β-actin loading controls. Color images available online at www.liebertpub.com/tea

angiopoietins or angiopoietins not regulating network formation under these conditions.

hES-MC integrate into a perivascular position in vivo

From our previous work we have shown that hES-MC have the capacity to stabilize and make heterotypic contact with ECs,[44] but they do not appear to take up a position of integration into the network wall *in vitro*, suggesting an immature state of assembly. Therefore, we asked whether the implantation microenvironment would induce integration of hES-MC into the vessel wall. HUVEC-DsRed and hES-MC-GFP were placed in coculture for 3 days and then implanted subcutaneously on the backs of immune compromised Rag1 mice for 1 week (Fig. 8). The constructs were examined by confocal microscopy at 40×, the series stacks were volume rendered into 3D images, and the percent volume overlap was calculated as described in the "Materials and Methods" section (Supplementary Figs. S3 and S4). Within 1 week, HUVEC assembled into vessel-like structures with hES-MC recruited to the wall (Fig. 8A, Merge–arrows). The hES-MC positioned themselves in an elongated configuration in parallel with the HUVEC network. Although some hES-MC remained resident in the bulk matrix, most appeared associated with the vessel-like structures. Quantification of the contact between the two cell types (Fig. 8B; cell overlap/HUVEC volume) indicated 13.6% ± 1.6% of HUVEC volume was shared with hES-MC while 17.2% ± 3.1% of hES-MC volume was shared with HUVEC (Fig. 8B; overlap/hES-MC). This data suggests that hES-MC posses the capacity to associate with a vessel wall and function as an MC *in vivo*.

Discussion

The main and novel findings of this study are as follows: (1) hES-MC participate with HUVEC to form an immature vascular-plexus-like structure *in vitro*, (2) hESC-derived mesenchymal cells express the vascular stabilizing factors HGF and Ang1, (3) HGF plays a significant role in hES-MC-HUVEC network assembly and stability, and (4) hES-MC can integrate into the vessel wall and function as an MC *in vivo*.

Providing a functional vasculature is a key requirement for the development of a therapeutic organoid and though we know many of the factors involved in vessel assembly, we still have major gaps in our understanding such that we cannot engineer stable, mature vascular systems at will.[67,68] Though some success in forming vessel structures has been achieved with ECs alone, it is clear that multicellular approaches in 3D architectures are ultimately required.[35,69,70] Thus, we need human cell sources that can accurately recapitulate the biological processes we are trying to control and manipulate for our purposes.[35] To this end, the perivascular cell in the microvasculature is of particular interest for our discipline as it is a critical component of the vascular tree that metabolically sustains the organ.[71,72] Because the functional characteristics of hES-MC parallel those of

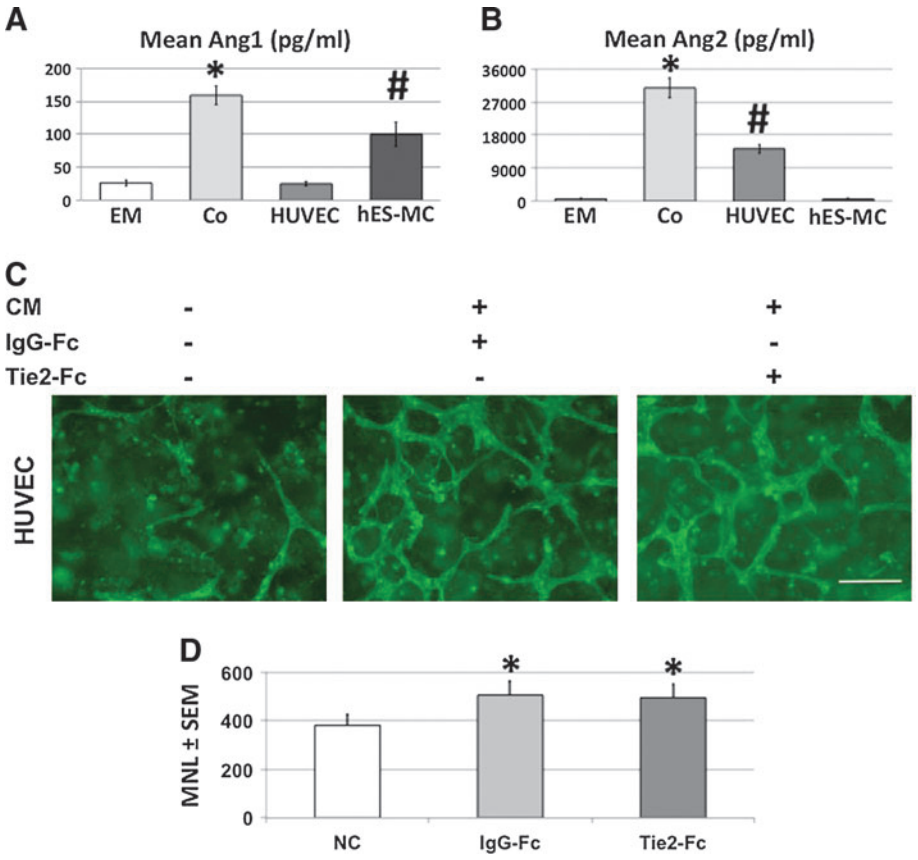

FIG. 7. Angiopoietin1/2 expression by HUVEC and hES-MC. ELISA analysis for expression of **(A)** Ang1 and **(B)** Ang2 for EM control, conditioned EM from coculture of HUVEC and hES-MC, HUVEC alone, or hES-MC alone. EM registered background levels of 26 ± 5 pg/mL and 622 ± 101 pg/mL, while coculture (Co) measured 159 ± 15 pg/mL and $30{,}867 \pm 2685$ pg/mL, which were both significantly greater than EM control (*$p = 0.004$ and 0.01). Conditioned media from HUVEC alone were not different compared with EM control for Ang1 (25 ± 4 pg/mL) but showed significantly more expression of Ang2 than EM control ($30{,}867 \pm 2685$ pg/mL, $^{\#}p = 0.01$). In contrast, conditioned media from hES-MC alone were significantly enriched in Ang1 (100 ± 18 pg/mL, $^{\#}p = 0.02$) but not in Ang2 (600 ± 144 pg/mL). **(C)** HUVEC were seeded in collagen-Fn gels at 10^6/mL and cultured in EM only (*left*), CM incubated with IgG-Fc (*middle*), or CM incubated with Tie2-Fc (*right*). **(D)** Mean network length quantification (±SEM) and one-way ANOVA indicate that exposure to hES-MC CM significantly increased network formation compared with EM control (*$p > 0.05$), but no significant difference was detected by treatment with Tie2-Fc (494 ± 58 μm) compared with IgG-Fc (505 ± 59 μm) control ($p = 0.4$) (HUVEC UEA-fluorescein, $n = 3$; 10×, scale bar = 200 μm). Color images available online at www.liebertpub.com/tea

MSCs and perivascular cells, we hypothesized that hES-MC are perivascular progenitor cells and tested them accordingly.[43,44]

Perivascular cells, both smooth muscle and pericytes, are enigmatic in part because of their uncertain lineage and lack of specific markers.[7,73–75] We have demonstrated previously that hES-MC are responsive to TGFβ1 and PDGF-B signaling.[44] Here we show that hES-MC express a battery of markers associated with perivascular cells, CD146,[29,30] EphB2,[76] NG2,[77] and Cx43.[78] This of itself does not prove that hES-MC are perivascular progenitors, but if one was seeking this progenitor *in vivo*, a reasonable expectation might be to detect their expression.

Vessels assemble in several identified steps, including EC proliferation and migration by VEGF and bFGF, MC recruitment through PDGF-B, MC differentiation through TGFβ1, vessel stabilization by Ang1, and destabilization by Ang2.[20] Though these mechanisms play leading roles in vascularization, it is unclear how these processes interact and what other mechanisms may be involved. Although bFGF and VEGF are robust angiogenic inducers,[79,80] they are insufficient to maintain HUVEC networks[44,55,81]; though recently Stratman and coworkers demonstrated that preculture with VEGF and bFGF was required for cytokine stabilization of cocultured EC-MCs.[82] HGF is a pleiotropic factor expressed by mesenchymal cells to affect Met-expressing epithelial/ECs.[83,84] HGF is angiogenic[85]; mediates pro-survival,[86] tubulogenesis,[87,88] and cell migration[83]; and can be oncogenic.[89] Xin *et al.*[90] demonstrated that HUVEC alone can survive in 3D collagen *in vitro* in the combined presence of very high VEGF and HGF (up to 200 ng/mL each). They also showed transcript upregulation of the pro-survival Bcl-2 family members A1 and Bcl-2. Our results indicate that HGF plays a stabilizing role in assembly of network structures.

Both Ang1 (hES-MC) and Ang2 (HUVEC)[91] are expressed in the coculture; however, in spite of being angiogenic, Ang2 is insufficient to stabilize HUVEC networks and the copious quantities may even play a role in HUVEC death.[42,55] It is

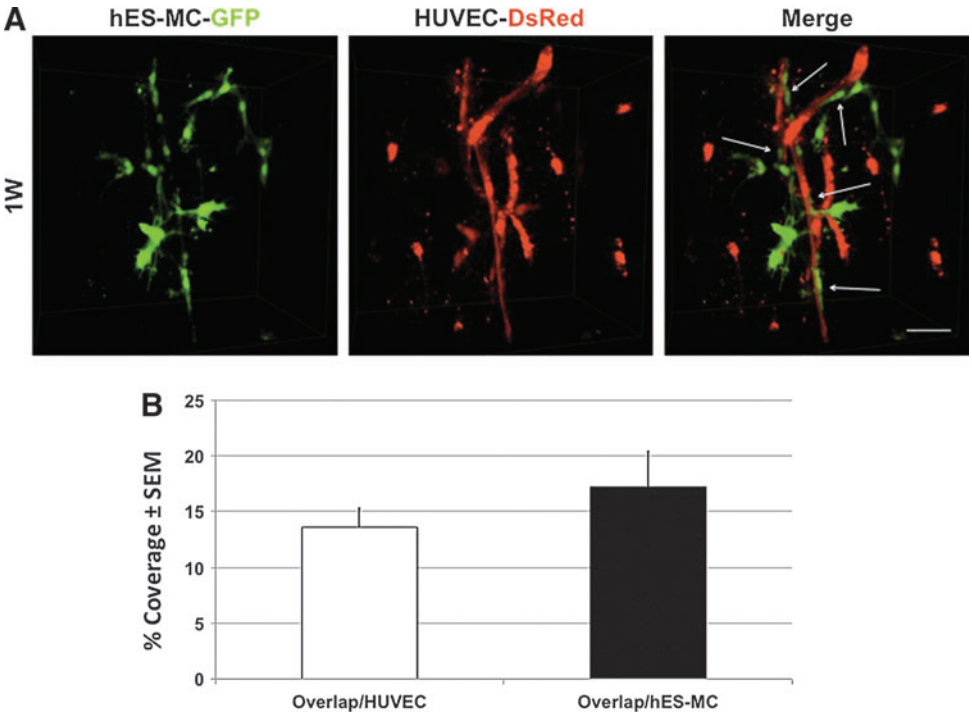

FIG. 8. hES-MC contact with EC networks *in vivo*. **(A)** HUVEC-DsRed and hES-MC-GFP (2×10^6:0.4×10^6/mL) were cocultured in GFR-Matrigel for 3 days *in vitro* before subcutaneous implantation in the back of Rag1 immune compromised mice for 1 week. Constructs were harvested and images were acquired by confocal microscopy and stack volume rendering. hES-MC integrate into EC networks that were formed *in vivo* (arrows). **(B)** Quantification of the percentage of direct cell contact with respect to HUVEC (cell overlap/HUVEC volume) and direct cell contact with respect to hES-MC (cell overlap/hES-MC volume) (40×, scale bar = 50 μm). Color images available online at www.liebertpub.com/tea

unclear how HGF and Ang1 from hES-MC may be interacting to stabilize HUVEC networks, but these results indicate that multiple factors are regulating these events. Identifying and understanding how these factors interact temporally and spatially will be key to engineer an effective vascularization environment.

Our data indicate that, under the environmental conditions examined, the networks resembled an immature capillary plexus and though we have demonstrated by high-resolution microscopy and image analysis ECs and hES-MC direct heterotypic contact,[44] hES-MC do not integrate into the vessel-like structures *in vitro* as in native vessels.[29,44] However, when HUVEC and hES-MC are precultured to initiate assembly and then implanted subcutaneously, hES-MC attached to the forming vessel and positioned themselves in an integrated location. In our previous work,[44] the *in vitro* contact percentage of HUVEC on hES-MC ranged from 3% to 12% while hES-MC on HUVEC was 2%–7%. Here, the implanted coculture percent contact of hES-MC on HUVEC increased to 12%–15% with HUVEC on hES-MC contact increasing to 14%–20%, indicating that hES-MC are capable of responding to factors within the *in vivo* environment that induce maturation signals (e.g., interstitial flow[92]). It also suggests that hES-MC can undergo the entire process of recruitment to vessel maturation making it potentially useful as a microvascular MC source for therapeutic applications. Thus, hES-MC may be a robust source of microvascular MCs for therapeutic or drug testing applications.[34,35]

Acknowledgments

Funds for this work were provided by University of Louisville, School of Medicine (N.L.B.), NCRR IDeA Awards INBRE-P20 RR016481 and COBRE-P20RR018733, and NIH EB007556 (J.B.H.).

Disclosure Statement

No competing financial interests exist.

References

1. D'Amore, P.A. Capillary growth: a two-cell system. Semin Cancer Biol **3,** 49, 1992.
2. Jin, S.W., and Patterson, C. The opening act: vasculogenesis and the origins of circulation. Arterioscler Thromb Vasc Biol **29,** 623, 2009.
3. Risau, W., and Flamme, I. Vasculogenesis. Annu Rev Cell Dev Biol **11,** 73, 1995.
4. Sabin, F.R. Studies on the origin of blood-vessels and of red blood-corpuscles as seen in the living blastoderm of chicks during the second day of incubation. Anat Rec **13,** 199, 1917.
5. Furuta, C., Ema, H., Takayanagi, S., Ogaeri, T., Okamura, D., Matsui, Y., *et al.* Discordant developmental waves of angioblasts and hemangioblasts in the early gastrulating mouse embryo. Development **133,** 2771, 2006.
6. Verma, A., Bhattacharya, R., Remadevi, I., Li, K., Pramanik, K., Samant, G.V., *et al.* Endothelial cell-specific chemotaxis receptor (ecscr) promotes angioblast migration during vasculogenesis and enhances VEGF receptor sensitivity. Blood **115,** 4614, 2010.
7. Majesky, M.W. Developmental basis of vascular smooth muscle diversity. Arterioscler Thromb Vasc Biol **27,** 1248, 2007.
8. Diaz-Flores, L., Gutierrez, R., Madrid, J.F., Varela, H., Valladares, F., Acosta, E., *et al.* Pericytes. Morphofunction, interactions and pathology in a quiescent and activated mesenchymal cell niche. Histol Histopathol **24,** 909, 2009.
9. Bergwerff, M., Verberne, M.E., DeRuiter, M.C., Poelmann, R.E., and Gittenberger-de, G.A.C. Neural crest cell contribution to the developing circulatory system: implications for vascular morphology? Circ Res **82,** 221, 1998.
10. Etchevers, H.C., Vincent, C., Le, D.N.M., and Couly, G.F. The cephalic neural crest provides pericytes and smooth

muscle cells to all blood vessels of the face and forebrain. Development **128,** 1059, 2001.
11. Dettman, R.W., Denetclaw, W., Jr., Ordahl, C.P., and Bristow, J. Common epicardial origin of coronary vascular smooth muscle, perivascular fibroblasts, and intermyocardial fibroblasts in the avian heart. Dev Biol **193,** 169, 1998.
12. Mikawa, T., and Gourdie, R.G. Pericardial mesoderm generates a population of coronary smooth muscle cells migrating into the heart along with ingrowth of the epicardial organ. Dev Biol **174,** 221, 1996.
13. Miano, J.M., Cserjesi, P., Ligon, K.L., Periasamy, M., and Olson, E.N. Smooth muscle myosin heavy chain exclusively marks the smooth muscle lineage during mouse embryogenesis. Circ Res **75,** 803, 1994.
14. Olson, L.E., and Soriano, P. PDGFRbeta signaling regulates mural cell plasticity and inhibits fat development. Dev Cell **20,** 815, 2011.
15. Seliktar, D., Black, R.A., Vito, R.P., and Nerem, R.M. Dynamic mechanical conditioning of collagen-gel blood vessel constructs induces remodeling *in vitro*. Ann Biomed Eng **28,** 351, 2000.
16. Gabbiani, G., Schmid, E., Winter, S., Chaponnier, C., de, C.C., Vandekerckhove, J., *et al.* Vascular smooth muscle cells differ from other smooth muscle cells: predominance of vimentin filaments and a specific alpha-type actin. Proc Natl Acad Sci U S A **78,** 298, 1981.
17. Duband, J.L., Gimona, M., Scatena, M., Sartore, S., and Small, J.V. Calponin and SM 22 as differentiation markers of smooth muscle: spatiotemporal distribution during avian embryonic development. Differentiation **55,** 1, 1993.
18. Sims, D.E., and Westfall, J.A. Analysis of relationships between pericytes and gas exchange capillaries in neonatal and mature bovine lungs. Microvasc Res **25,** 333, 1983.
19. Sims, D.E., Miller, F.N., Donald, A., and Perricone, M.A. Ultrastructure of pericytes in early stages of histamine-induced inflammation. J Morphol **206,** 333, 1990.
20. Armulik, A., Abramsson, A., and Betsholtz, C. Endothelial/pericyte interactions. Circ Res **97,** 512, 2005.
21. Hirschi, K.K., Rohovsky, S.A., and D'Amore, P.A. PDGF, TGF-beta, and heterotypic cell-cell interactions mediate endothelial cell-induced recruitment of 10T1/2 cells and their differentiation to a smooth muscle fate. J Cell Biol **141,** 805, 1998.
22. Herman, I.M., and D'Amore, P.A. Microvascular pericytes contain muscle and nonmuscle actins. J Cell Biol **101,** 43, 1985.
23. Stratman, A.N., Malotte, K.M., Mahan, R.D., Davis, M.J., and Davis, G.E. Pericyte recruitment during vasculogenic tube assembly stimulates endothelial basement membrane matrix formation. Blood **114,** 5091, 2009.
24. Sinha, S., Wamhoff, B.R., Hoofnagle, M.H., Thomas, J., Neppl, R.L., Deering, T., *et al.* Assessment of contractility of purified smooth muscle cells derived from embryonic stem cells. Stem Cells **24,**1678, 2006.
25. Vo, E., Hanjaya-Putra, D., Zha, Y., Kusuma, S., and Gerecht, S. Smooth-muscle-like cells derived from human embryonic stem cells support and augment cord-like structures in vitro. Stem Cell Rev **6,** 237, 2010.
26. Ross, R., Everett, N.B., and Tyler, R. Wound healing and collagen formation. VI. The origin of the wound fibroblast studied in parabiosis. J Cell Biol **44,** 645, 1970.
27. Canfield, A.E., Sutton, A.B., Hoyland, J.A., and Schor, A.M. Association of thrombospondin-1 with osteogenic differentiation of retinal pericytes *in vitro*. J Cell Sci **109(Pt 2),** 343, 1996.
28. Schor, A.M., Canfield, A.E., Sutton, A.B., Arciniegas, E., and Allen, T.D. Pericyte differentiation. Clin Orthop Relat Res **313,** 81, 1995.
29. Crisan, M., Yap, S., Casteilla, L., Chen, C.W., Corselli, M., Park, T.S., *et al.* A perivascular origin for mesenchymal stem cells in multiple human organs. Cell Stem Cell **3,** 301, 2008.
30. Covas, D.T., Panepucci, R.A., Fontes, A.M., Silva, W.A., Jr., Orellana, M.D., Freitas, M.C., *et al.* Multipotent mesenchymal stromal cells obtained from diverse human tissues share functional properties and gene-expression profile with CD146+ perivascular cells and fibroblasts. Exp Hematol **36,** 642, 2008.
31. Pittenger, M.F., Mackay, A.M., Beck, S.C., Jaiswal, R.K., Douglas, R., Mosca, J.D., *et al.* Multilineage potential of adult human mesenchymal stem cells. Science **284,**143, 1999.
32. Bosch, P., Pratt, S.L., and Stice, S.L. Isolation, characterization, gene modification, and nuclear reprogramming of porcine mesenchymal stem cells. Biol Reprod **74,** 46, 2006.
33. Caplan, A.I. All MSCs are pericytes? Cell Stem Cell **3,** 229, 2008.
34. Nunes, S.S., Song, H., Chiang, C.K., and Radisic, M. Stem cell-based cardiac tissue engineering. J Cardiovasc Transl Res **4,** 592, 2011.
35. Au, P., Tam, J., Duda, D.G., Lin, P.C., Munn, L.L., Fukumura, D., *et al.* Paradoxical effects of PDGF-BB overexpression in endothelial cells on engineered blood vessels *in vivo*. Am J Pathol **175,** 294, 2009.
36. Koike, N., Fukumura, D., Gralla, O., Au, P., Schechner, J.S., and Jain, R.K. Tissue engineering: creation of long-lasting blood vessels. Nature **428,** 138, 2004.
37. Hellstrom, M., Kalen, M., Lindahl, P., Abramsson, A., and Betsholtz, C. Role of PDGF-B and PDGFR-beta in recruitment of vascular smooth muscle cells and pericytes during embryonic blood vessel formation in the mouse. Development **126,** 3047, 1999.
38. Dickson, M.C., Martin, J.S., Cousins, F.M., Kulkarni, A.B., Karlsson, S., and Akhurst, R.J. Defective haematopoiesis and vasculogenesis in transforming growth factor-beta 1 knock out mice. Development **121,** 1845, 1995.
39. Larsson, J., Goumans, M.J., Sjostrand, L.J., van Rooijen, M.A., Ward, D., Leveen, P., *et al.* Abnormal angiogenesis but intact hematopoietic potential in TGF-beta type I receptor-deficient mice. EMBO J **20,** 1663, 2001.
40. Thurston, G., Suri, C., Smith, K., McClain, J., Sato, T.N., Yancopoulos, G.D., *et al.* Leakage-resistant blood vessels in mice transgenically overexpressing angiopoietin-1. Science **286,** 2511, 1999.
41. Thurston, G., Rudge, J.S., Ioffe, E., Zhou, H., Ross, L., Croll, S.D., *et al.* Angiopoietin-1 protects the adult vasculature against plasma leakage. Nat Med **6,** 460, 2000.
42. Scharpfenecker, M., Fiedler, U., Reiss, Y., and Augustin, H.G. The Tie-2 ligand angiopoietin-2 destabilizes quiescent endothelium through an internal autocrine loop mechanism. J Cell Sci **118,** 771, 2005.
43. Boyd, N.L., Robbins, K.R., Dhara, S.K., West, F.D., and Stice, S.L. Human Embryonic Stem Cell-Derived Mesoderm-like Epithelium Transitions to Mesenchymal Progenitor Cells. Tissue Eng Part A **15,** 1897, 2009.
44. Boyd, N.L., Nunes, S.S., Jokinen, J.D., Krishnan, L., Chen, Y., Smith, K.H., *et al.* Microvascular mural cell functionality of human embryonic stem cell-derived mesenchymal cells. Tissue Eng Part A **17,** 1537, 2011.

45. Kitamura, T., Koshino, Y., Shibata, F., Oki, T., Nakajima, H., Nosaka, T., *et al.* Retrovirus-mediated gene transfer and expression cloning: powerful tools in functional genomics. Exp Hematol **31,** 1007, 2003.
46. Morgenstern, J.P., and Land, H. Advanced mammalian gene transfer: high titre retroviral vectors with multiple drug selection markers and a complementary helper-free packaging cell line. Nucleic Acids Res **18,** 3587, 1990.
47. Gupta, P.B., Kuperwasser, C., Brunet, J.P., Ramaswamy, S., Kuo, W.L., Gray, J.W., *et al.* The melanocyte differentiation program predisposes to metastasis after neoplastic transformation. Nat Genet **37,** 1047, 2005.
48. Livak, K.J., and Schmittgen, T.D. Analysis of relative gene expression data using real-time quantitative PCR and the 2(-Delta Delta C(T)) Method. Methods **25,** 402, 2001.
49. Harfouche, R., Malak, N.A., Brandes, R.P., Karsan, A., Irani, K., and Hussain, S.N. Roles of reactive oxygen species in angiopoietin-1/tie-2 receptor signaling. FASEB J **19,** 1728, 2005.
50. Nunes, S.S., Greer, K.A., Stiening, C.M., Chen, H.Y., Kidd, K.R., Schwartz, M.A., *et al.* Implanted microvessels progress through distinct neovascularization phenotypes. Microvasc Res **79,** 10, 2009.
51. Krishnan, L., Underwood, C.J., Maas, S., Ellis, B.J., Kode, T.C., Hoying, J.B., *et al.* Effect of mechanical boundary conditions on orientation of angiogenic microvessels. Cardiovasc Res **78,** 324, 2008.
52. Nunes, S.S., Krishnan, L., Gerard, C.S., Dale, J.R., Maddie, M.A., Benton, R.L., *et al.* Angiogenic potential of microvessel fragments is independent of the tissue of origin and can be influenced by the cellular composition of the implants. Microcirculation **17,** 557, 2010.
53. Liu, Y., Wilkinson, F.L., Kirton, J.P., Jeziorska, M., Iizasa, H., Sai, Y., *et al.* Hepatocyte growth factor and c-Met expression in pericytes: implications for atherosclerotic plaque development. J Pathol **212,** 12, 2007.
54. Goto, F., Goto, K., Weindel, K., and Folkman, J. Synergistic effects of vascular endothelial growth factor and basic fibroblast growth factor on the proliferation and cord formation of bovine capillary endothelial cells within collagen gels. Lab Invest **69,** 508, 1993.
55. Ilan, N., Mahooti, S., and Madri, J.A. Distinct signal transduction pathways are utilized during the tube formation and survival phases of *in vitro* angiogenesis. J Cell Sci **111(Pt 24),** 3621, 1998.
56. Wang, X., Le, P., Liang, C., Chan, J., Kiewlich, D., Miller, T., *et al.* Potent and selective inhibitors of the Met [hepatocyte growth factor/scatter factor (HGF/SF) receptor] tyrosine kinase block HGF/SF-induced tumor cell growth and invasion. Mol Cancer Ther **2,** 1085, 2003.
57. Giannoni, P., Scaglione, S., Quarto, R., Narcisi, R., Parodi, M., Balleari, E., *et al.* An interaction between hepatocyte growth factor and its receptor (c-MET) prolongs the survival of chronic lymphocytic leukemic cells through STAT3 phosphorylation: a potential role of mesenchymal cells in the disease. Haematologica **96,** 1015, 2011.
58. Rong, S., Segal, S., Anver, M., Resau, J.H., and Vande, W.G.F. Invasiveness and metastasis of NIH 3T3 cells induced by Met-hepatocyte growth factor/scatter factor autocrine stimulation. Proc Natl Acad Sci U S A **91,** 4731, 1994.
59. Heideman, D.A., Overmeer, R.M., van BVW, Lamers, W.H., Hakvoort, T.B., Snijders, P.J., *et al.* Inhibition of angiogenesis and HGF-cMET-elicited malignant processes in human hepatocellular carcinoma cells using adenoviral vector-mediated NK4 gene therapy. Cancer Gene Ther **12,** 954, 2005.
60. Morisako, T., Takahashi, K., Kishi, K., Kiguchi, T., Mikami, R., Kobayashi, K., *et al.* Production of hepatocyte growth factor from human lung microvascular endothelial cells induced by interleukin-1beta. Exp Lung Res **27,** 675, 2001.
61. Trusolino, L., Bertotti, A., and Comoglio, P.M. MET signalling: principles and functions in development, organ regeneration and cancer. Nat Rev Mol Cell Biol **11,** 834, 2010.
62. Dumont, D.J., Gradwohl, G., Fong, G.H., Puri, M.C., Gertsenstein, M., Auerbach, A., *et al.* Dominant-negative and targeted null mutations in the endothelial receptor tyrosine kinase, tek, reveal a critical role in vasculogenesis of the embryo. Genes Dev **8,** 1897, 1994.
63. Suri, C., Jones, P.F., Patan, S., Bartunkova, S., Maisonpierre, P.C., Davis, S., *et al.* Requisite role of angiopoietin-1, a ligand for the TIE2 receptor, during embryonic angiogenesis. Cell **87,** 1171, 1996.
64. Takakura, N., Huang, X.L., Naruse, T., Hamaguchi, I., Dumont, D.J., Yancopoulos, G.D., *et al.* Critical role of the TIE2 endothelial cell receptor in the development of definitive hematopoiesis. Immunity **9,** 677, 1998.
65. Koblizek, T.I., Weiss, C., Yancopoulos, G.D., Deutsch, U., and Risau, W. Angiopoietin-1 induces sprouting angiogenesis *in vitro*. Curr Biol **8,** 529, 1998.
66. Teichert-Kuliszewska, K., Maisonpierre, P.C., Jones, N., Campbell, A.I., Master, Z., Bendeck, M.P., *et al.* Biological action of angiopoietin-2 in a fibrin matrix model of angiogenesis is associated with activation of Tie2. Cardiovasc Res **49,** 659, 2001.
67. Johnson, P.C., Mikos, A.G., Fisher, J.P., and Jansen, J.A. Strategic directions in tissue engineering. Tissue Eng **13,** 2827, 2007.
68. Langer, R. Tissue engineering: perspectives, challenges, and future directions. Tissue Eng **13,** 1, 2007.
69. Folkman, J., and Hochberg, M. Self-regulation of growth in three dimensions. J Exp Med **138,** 745, 1973.
70. Davis, G.E., Koh, W., and Stratman, A.N. Mechanisms controlling human endothelial lumen formation and tube assembly in three-dimensional extracellular matrices. Birth Defects Res C Embryo Today **81,** 270, 2007.
71. Gersh, I., and Still, M.A. Blood Vessels in Fat Tissue. Relation to Problems of Gas Exchange. J Exp Med **81,** 219, 1945.
72. Rupnick, M.A., Panigrahy, D., Zhang, C.Y., Dallabrida, S.M., Lowell, B.B., Langer, R., *et al.* Adipose tissue mass can be regulated through the vasculature. Proc Natl Acad Sci U S A **99,** 10730, 2002.
73. Armulik, A., Genove, G., and Betsholtz, C. Pericytes: developmental, physiological, and pathological perspectives, problems, and promises. Dev Cell **21,** 193, 2011.
74. Dore-Duffy, P. Pericytes: pluripotent cells of the blood brain barrier. Curr Pharm Des **14,** 1581, 2008.
75. Drake, C.J., Hungerford, J.E., and Little, C.D. Morphogenesis of the first blood vessels. Ann N Y Acad Sci **857,**155, 1998.
76. Salvucci, O., Maric, D., Economopoulou, M., Sakakibara, S., Merlin, S., Follenzi, A., *et al.* EphrinB reverse signaling contributes to endothelial and mural cell assembly into vascular structures. Blood **114,** 1707, 2009.
77. Ozerdem, U., Grako, K.A., Dahlin-Huppe, K., Monosov, E., and Stallcup, W.B. NG2 proteoglycan is expressed exclusively by mural cells during vascular morphogenesis. Dev Dyn **222,** 218, 2001.
78. Larson, D.M., Carson, M.P., and Haudenschild, C.C. Junctional transfer of small molecules in cultured bovine brain microvascular endothelial cells and pericytes. Microvasc Res **34,** 184, 1987.

79. Hoying, J.B., and Williams, S.K. Effects of basic fibroblast growth factor on human microvessel endothelial cell migration on collagen I correlates inversely with adhesion and is cell density dependent. J Cell Physiol **168,** 294, 1996.
80. Leung, D.W., Cachianes, G., Kuang, W.J., Goeddel, D.V., and Ferrara, N. Vascular endothelial growth factor is a secreted angiogenic mitogen. Science **246,** 1306, 1989.
81. Bayless, K.J., Salazar, R., and Davis, G.E. RGD-dependent vacuolation and lumen formation observed during endothelial cell morphogenesis in three-dimensional fibrin matrices involves the alpha(v)beta(3) and alpha(5)beta(1) integrins. Am J Pathol **156,** 1673 2000.
82. Stratman, A.N., Davis, M.J., and Davis, G.E. VEGF and FGF prime vascular tube morphogenesis and sprouting directed by hematopoietic stem cell cytokines. Blood **117,** 3709, 2011.
83. Stoker, M., and Perryman, M. An epithelial scatter factor released by embryo fibroblasts. J Cell Sci **77,** 209, 1985.
84. Rubin, J.S., Chan, A.M., Bottaro, D.P., Burgess, W.H., Taylor, W.G., Cech, A.C., *et al.* A broad-spectrum human lung fibroblast-derived mitogen is a variant of hepatocyte growth factor. Proc Natl Acad Sci U S A **88,** 415, 1991.
85. Sengupta, S., Gherardi, E., Sellers, L.A., Wood, J.M., Sasisekharan, R., and Fan, T.P. Hepatocyte growth factor/scatter factor can induce angiogenesis independently of vascular endothelial growth factor. Arterioscler Thromb Vasc Biol **23,** 69, 2003.
86. Fan, S., Ma, Y.X., Wang, J.A., Yuan, R.Q., Meng, Q., Cao, Y., *et al.* The cytokine hepatocyte growth factor/scatter factor inhibits apoptosis and enhances DNA repair by a common mechanism involving signaling through phosphatidyl inositol 3′ kinase. Oncogene **19,** 2212, 2000.
87. Montesano, R., Soriano, J.V., Malinda, K.M., Ponce, M.L., Bafico, A., Kleinman, H.K., *et al.* Differential effects of hepatocyte growth factor isoforms on epithelial and endothelial tubulogenesis. Cell Growth Differ **9,** 355, 1998.
88. Tsarfaty, I., Resau, J.H., Rulong, S., Keydar, I., Faletto, D.L., and Vande, W.G.F. The met proto-oncogene receptor and lumen formation. Science **257,** 1258, 1992.
89. Furge, K.A., Kiewlich, D., Le, P., Vo, M.N., Faure, M., Howlett, A.R., *et al.* Suppression of Ras-mediated tumorigenicity and metastasis through inhibition of the Met receptor tyrosine kinase. Proc Natl Acad Sci U S A **98,** 10722, 2001.
90. Xin, X., Yang, S., Ingle, G., Zlot, C., Rangell, L., Kowalski, J., *et al.* Hepatocyte growth factor enhances vascular endothelial growth factor-induced angiogenesis *in vitro* and *in vivo*. Am J Pathol **158,** 1111, 2001.
91. Jang, C., Koh, Y.J., Lim, N.K., Kang, H.J., Kim, D.H., Park, S.K., *et al.* Angiopoietin-2 exocytosis is stimulated by sphingosine-1-phosphate in human blood and lymphatic endothelial cells. Arterioscler Thromb Vasc Biol **29,** 401, 2009.
92. Helm, C.L., Fleury, M.E., Zisch, A.H., Boschetti, F., and Swartz, M.A. Synergy between interstitial flow and VEGF directs capillary morphogenesis *in vitro* through a gradient amplification mechanism. Proc Natl Acad Sci U S A **102,** 15779, 2005.

Address correspondence to:
Nolan L. Boyd, Ph.D.
Cardiovascular Innovation Institute
University of Louisville
302 E Muhammad Ali Blvd
Louisville, KY 40202

E-mail: nolan.boyd@louisville.edu

Received: July 19, 2011
Accepted: July 30, 2012
Online Publication Date: September 11, 2012